Spectral hole burning in Eu^{3+}-doped highly porous γ-aluminum oxide

S. P. Feofilov, A. A. Kaplyanskii, and R. I. Zakharchenya
A. F. Ioffe Physical-Technical Institute, 194021, St. Petersburg, Russia

Y. Sun, K. W. Jang, and R. S. Meltzer
Department of Physics and Astronomy, The University of Georgia, Athens, Georgia 30602

(Received 15 April 1996)

Transient and persistent spectral holes were burned in the $^7F_0$-$^5D_0$ transition of Eu^{3+} ions in macromonolithic transparent porous nanocrystalline γ-Al_2O_3 produced by sol-gel technology. An unusual temperature dependence of the transient hole width was observed that differs markedly from that in either crystalline or disordered systems. This temperature dependence is explained in terms of Raman processes involving size-resonant vibrations of the nanoparticles comprising the structure. Possible mechanisms of hole burning are suggested. [S0163-1829(96)52730-X]

I. INTRODUCTION

Studies of spatially restricted solids whose dimensions are on the nanometer scale, exhibit the effects of size confinement on their vibrational properties (Refs. 1–3 and references therein). These altered vibrational properties can be expected to result in modifications of those spectroscopic properties of impurity ions in a nanocrystalline insulating host which depend on the electron-phonon interaction. A well-known example occurs in glasses[4] and disordered crystals[5] where the homogeneous linewidths are much larger than and their temperature dependence is fundamentally different from those in regular crystals. These effects are connected with specific vibrational properties of glasses (and disordered crystals), such as localization of vibrational excitations and the presence of two-level systems (TLS's).

In the present work optical hole-burning spectroscopy is used to study the dynamics of impurity ions in nanocrystalline highly porous transparent γ-Al_2O_3:Eu^{3+} produced by sol-gel technology. Both transient and persistent hole burning is observed. The transient hole linewidth exhibits an abrupt increase in its temperature dependence above 7 K which is interpreted on the basis of the recently observed[6] modification of the vibrational spectrum of the nanoscale material.

The macromonolithic translucent porous aluminum oxide samples, γ-Al_2O_3:Eu^{3+}, with an Eu concentration of 1 and 2 at %, were produced by the sol-gel technique.[7,8] The material is built of nanometer scale crystalline particles. Their crystal structure was probed by x-ray scattering. The apparent density of the samples, which is less than half that of bulk γ-Al_2O_3, confirms their high porosity. The average diameter of the crystalline nanoparticles was about 4 nm based on x-ray scattering data. The typical spread in the mean particle size distribution is of the order of the size itself (± 2 nm). For these Eu concentrations each nanoparticle contains 20–40 Eu ions.

In the spinel-type γ-Al_2O_3 structure, the Al^{3+} ions occupy the tetrahedral and octahedral sites statistically, so the γ-Al_2O_3 lattice is a defect (disordered) one. Thus the spectroscopic properties of Eu^{3+} in the samples are expected to be typical for disordered materials.

The nonresonantly excited fluorescence spectrum of Eu^{3+} ions is shown in Fig. 1. It demonstrates the strong ($\sim$150 cm^{-1}) inhomogeneous broadening of all $^5D_0$-^7F_n transitions similar to that found in glasses[9] and highly disordered crystals.[5] The $^5D_0$-$^7F_0$ transition is observed at about 577 nm; the other spectral lines in Fig. 1 may be attributed to the $^5D_0$-$^7F_1$ and $^5D_0$-$^7F_2$ transitions whose splittings are similar to those of Eu^{3+} in other disordered hosts.[9] No significant nonresonant fluorescent line narrowing was observed in the $^5D_0$-$^7F_1$ and $^5D_0$-$^7F_2$ transitions under site-selective excitation of the $^7F_0$-$^5D_0$ transition, suggesting the absence of correlation between $^5D_0$-^7F_n energy levels in different Eu^{3+} sites. The fluorescence decay is nonexponential due to the different lifetimes of Eu^{3+} centers, typical for disordered materials, estimated as $\sim$1–2 ms at room temperature.

II. HOLE-BURNING EXPERIMENTS

The hole-burning experiments were performed at 1.7–40 K. A single-frequency ring dye-laser (Coherent model 899-

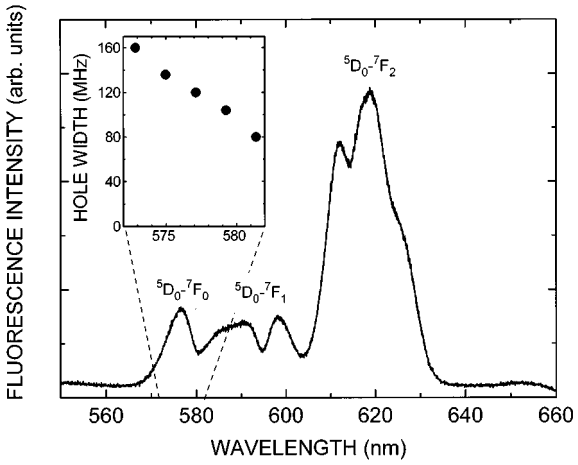

FIG. 1. The fluorescence spectrum at $T=77$ K of γ-Al_2O_3:Eu^{3+} produced by sol-gel technology under Hg-lamp excitation. Inset: spectral dependence of the transient hole width.

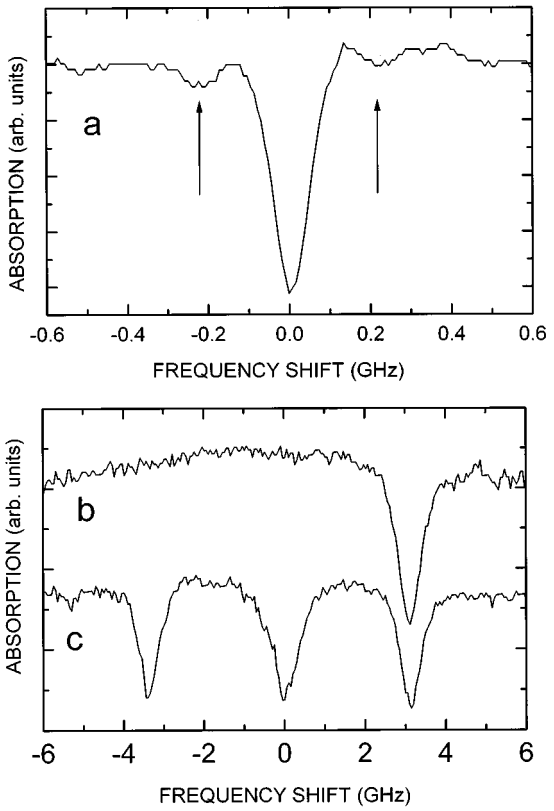

FIG. 2. Spectral holes burned in $^7F_0$-$^5D_0$ transition of Eu^{3+} ions at $T=1.8$ K. (a) Transient hole; (b) persistent hole; (c) multiple persistent holes. The arrows in (a) indicate the sideholes.

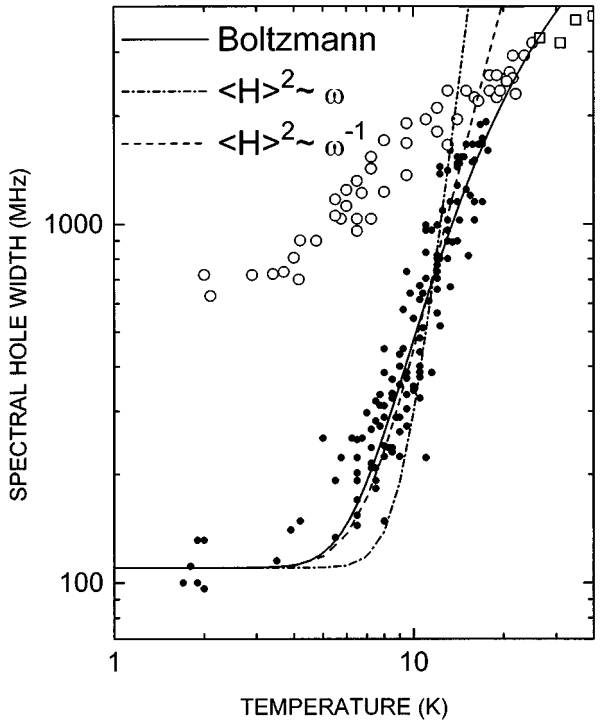

FIG. 3. Temperature dependencies of hole widths. Solid circles—transient hole; open circles and squares—persistent hole (data points shown with squares were obtained with additional burning at elevated temperatures); solid line—fit with Boltzmann activation; dash-dotted line—fit with Eq. (1) and $\langle H\rangle^2\sim\omega$; dashed line—fit with Eq. (1) and $\langle H\rangle^2\sim\omega^{-1}$.

21) was tuned into the $^7F_0$-$^5D_0$ transition. The laser power was 5–100 mW focused onto a 2–5 mm spot on the sample. For the hole detection the laser frequency was swept over a range which was adjusted between 2–20 GHz in a time period of ~0.5 s while the fluorescence in the $^5D_0$-$^7F_2$ transition (620 nm) was detected by a photomultiplier tube. The fluorescence around 620 nm was selected with a Corning 2-62 cutoff filter and a 10 nm bandwidth interference filter. A digital oscilloscope was used for signal storage and averaging.

Two kinds of spectral holes observed in our experiments are shown in Fig. 2. These are transient holes (lifetime~a few seconds) [Fig. 2(a)] and significantly broader persistent holes whose lifetime is greater than hours at $T=2$ K [Fig. 2(b)]. The transient holes were observed in a repetitive sequence in which the laser frequency was held fixed for 0.5 s, followed by a scan of the laser frequency in 0.5 s. In order to avoid persistent hole burning the laser power was kept below 5 mW and the spot size was at least 5 mm in diameter. The transient hole width was about 100 MHz at $T=1.7$ K in the center of the inhomogeneously broadened $^7F_0$-$^5D_0$ line and showed a linear excitation wavelength dependence (see inset of Fig. 1) similar to that observed in some glasses.[9] The maximum hole depth was about 10%. The transient holes exhibited some weakly resolved structure, which together with the hole lifetime suggests that the hole burning is due to redistribution of population among the hyperfine levels of the ground state as has been observed in a number of ordered[10] and disordered[5] crystals and in glasses.[9]

The persistent holes [Fig. 2(b)] were burned at $T=1.8$ K with laser powers between 5 and 100 mW, the larger powers being used at the higher temperatures, loosely focused onto a 2 mm spot. The hole width significantly increases with burning intensity. At low intensities (~10 mW at $T=1.7$ K) the hole width was about 600 MHz. The maximum observed hole depth was ~15% and the typical burning time was from seconds at higher intensities to tens of minutes under low-intensity conditions. The cycling of the sample to higher temperatures showed that at $T>20$ K the hole is irreversibly broadened and its area is decreased. The holes do not survive cycling above 40 K. The low activation energy of hole erasure suggests that the persistent holes are of photophysical origin (due to rearrangement of the material structure). Several persistent holes may be burned at different frequencies with the same laser beam position in the sample and each new hole does not affect the depth and the width of the previously burned holes as seen in Fig. 2(c).

The temperature dependence of the hole widths of both the transient and persistent holes, measured at 577 mn, are shown in Fig. 3. The temperature dependence for the narrow transient hole is very weak below 6 K but speeds up drastically at higher temperatures. The width of the persistent hole, initially burned at $T=2$ K, broadens nearly linearly as the temperature is increased although a somewhat slower dependence may be observed at low temperatures. It should be mentioned that in the case of persistent holes for the higher temperature points (open squares in Fig. 3) the holes were burned at the elevated temperature. Where the holes could be burned at both 1.8 K and the elevated temperatures, the results were identical within the experimental error. The results

of all the measurements were indistinguishable for the 1 and 2% Eu doped samples and therefore data for both concentrations are shown in Fig. 3.

III. DISCUSSION

The mechanism for the transient hole burning may be ascribed to the redistribution of population among the hyperfine ground-state sublevels which is active when the homogeneous linewidth is less than the ground-state hyperfine splittings. This is supported by the observation of sidehole structure close to the main hole. The hole spectra of Eu^{3+} then contain antiholes which are combinations of hyperfine splittings in the ground and excited state and sideholes which are determined by the excited-state hyperfine splittings. In octahedral oxide environments, Eu^{3+} usually exhibits hyperfine splittings of about $\sim$250 MHz in the ground state[10] and $\sim$500 MHz in the excited state. The presence of sidehole structure indicates that at least some of the sites have hyperfine splittings which exceed the homogeneous linewidth. The presence of overlapping holes and antiholes, with a distribution of frequencies from the main hole, washes out most of the structure. The transient hole lifetime also supports the proposed mechanism as its value of 10 s at 2 K is quite typical for that found in glasses and disordered materials.[9] The maximum hole depth of 10% may be related to the large homogeneous linewidth which restricts the persistent hole burning to sites whose hyperfine splittings exceed the homogeneous linewidth.

The exact nature of the mechanism for the persistent hole is not so clear. The relatively low activation temperature of the irreversible broadening and erasure of these holes is suggestive of a photophysical rearrangement of the local environment as has been ascribed to persistent hole burning of Pr^{3+} in glasses[9] and disordered solids.[11] While persistent spectral hole burning is usually not observed for Eu^{3+}, one other example is known to us in the superionic conductor, Na β'' alumina.[12] However in a porous nanocrystalline material the rearrangement of the nanocrystal as a whole provides an alternate mechanism. The nanoscale size restriction can enhance the effect of optical excitation as it provides a means for significant local heating of the nanocrystal. This heating has been estimated assuming the bulk heat capacity of the material and it was found that the energy of a single photon is enough to heat the nanocrystal to few tens of K. Experiments[6] have shown that the spectrum of optically excited vibrations is highly nonequilibrium and size-resonant vibrations of particles with long ($\sim$ms) lifetimes are effectively excited. This may result in rearrangement of the position of the nanocrystal with respect to its neighbors and thus in changes in nanocrystal stress which shifts the ions' frequency. The required energy may be provided by the phonons created in the Eu^{3+} transition to the vibronic ground state or by nonradiative relaxation to the ground state. The observation that burning of additional holes does not significantly affect those previously burned [see Fig. 2(c)] may be easily explained by the separation of the ions involved in the hole-burning processes in different nanoparticles which effectively do not interact.

The temperature dependence of the transient hole width $\Gamma(T)$, observed in γ-Al_2O_3:Eu^{3+} is quite unusual. Indeed, $\Gamma(T)$ is different from that of Eu^{3+} in ordered crystals where it follows a $\sim T^7$ behavior at low temperatures with the transition to $\sim T^2$ at higher temperatures,[13] and from that in glasses and disordered crystals where it is $\sim T$ to $T^{1.3}$ at low temperatures and $\sim T^2$ at higher temperatures.[4,9] The T^7 dependence obtained for Eu^{3+} in bulk crystalline Y_2O_3 was explained on the basis of a two-phonon Raman process. The seventh power follows from the ω^2 dependence of the phonon density of states. We consider the observed temperature dependence in terms of this same two-phonon Raman process taking into account the specific vibrational spectrum of the nanocrystalline material.[2] The Raman process gives a contribution

$$\Gamma \sim \int_{\omega_1}^{\omega_2} |\langle H \rangle|^4 \frac{\rho(\omega)^2 e^{\hbar\omega/kT}}{(e^{\hbar\omega/kT}-1)^2} d\omega \qquad (1)$$

for the interactions with the vibrations with frequencies lying between ω_1 and ω_2, where H is the electron-phonon interaction Hamiltonian and $\rho(\omega)$ is the vibrational density of states.[14] For nanocrystalline material the low-frequency ($<$20 cm^{-1}) density of states is decreased due to the size restricted boundaries of the nanocrystals; the additional density of states due to size-quantized particle vibrations is present at higher frequencies. The frequency spectrum of vibrations in small crystalline particles was considered in Refs. 2 and 15. The nanoparticle vibrations which are most responsible for the additional density of states are so-called ''surface'' spheroidal and torsional modes whose lowest frequency is

$$\omega \ (\mathrm{cm}^{-1}) = 0.85 v_t / ac, \qquad (2)$$

where v_t is the transverse sound velocity and a is the particle diameter.

We have made an attempt to fit the experimental results with Eq. (1) assuming $\langle H \rangle^2 \sim \omega$ (as is done for crystals) and the smoothed frequency spectrum of phonons for a mesoscopic system[15] for $\rho(\omega)$. The integration was performed between the lowest-lying 4-nm particle mode frequency and 700 cm^{-1}. It was not possible to explain the experimental results assuming a value of $\langle H \rangle^2 \sim \omega$ of the same order as that in bulk crystalline oxide materials;[13] the observed linewidth is a few orders of magnitude larger. In addition, the slope of the temperature dependence cannot be fitted, even assuming an increased value of $\langle H \rangle^2$ (still $\sim\omega$) (see Fig. 3, dash-dotted line). A better fit for the temperature dependence is obtained taking $\langle H \rangle^2 \sim \omega^{-1}$ (Fig. 3, dashed line) as is assumed for Raman processes involving the interaction with localized vibrations in glasses[16] (of course in this case the absolute value of $\langle H \rangle^2$ is just a fitting parameter). A good fit of the results is also obtained (Fig. 3, solid line) with a Boltzmann activation $e^{-\hbar\omega/kT}$ which corresponds to Raman processes involving vibrations with frequencies narrowly distributed around $\omega \approx 25$ cm^{-1}, the minimum frequency predicted for a particle with $a = 6$ nm. The use of a larger particle size can be justified because the larger particles contain more Eu^{3+} probe ions. Thus their contribution to the hole line shape is expected to dominate. An exponential temperature dependence of Γ was previously reported in the dye-surface system Quinizarin/γ-Al_2O_3 which was ascribed to some unknown low-frequency mode of the adsorbate-substrate system.[17] For

porous sol-gel γ-Al_2O_3 the exponential-like temperature behavior of Γ results from a gap in the low-frequency phonon spectrum with a sudden onset of size resonant modes at a frequency given by Eq. (2). This results in a temperature behavior like that observed for the dye-adsorbate system as well as for localized modes in glasses[14] and low-frequency vibrations of organic molecules.[18]

The fitting of the experimental data with Eq. (1) requires that the electron-vibration interaction responsible for the line broadening in nanocrystalline material is stronger than that in bulk crystals. There are two reasons why the nanoscale size restriction may enhance the line broadening. The first lies in the fact that this structure ensures that each Eu^{3+} ion is not more than about 2 nm from the surface of the particle where these modes are most active. Thus the nanoscale structure of the materials has the effect of increasing the effective electron-phonon interaction. In the second place, the density of states of these modes is really quite large at $\sim 25\ cm^{-1}$ as compared with the acoustic modes in a bulk crystal.

At the lowest temperatures the transient hole width is determined by some other mechanism, e.g., interaction with TLS's, which may be present in this defect lattice, with fractons,[1] or by spectral diffusion. The hole width for persistent holes should also exhibit some increased temperature dependence above $T=6$ K, but it is difficult to identify because at higher temperatures the persistent hole broadening is determined mostly by inhomogeneous broadening due to thermally activated rearrangements in the material. The irreversible character of the hole broadening at $T>20$ K supports this suggestion.

The nanocrystalline structure presents special conditions for spectral hole burning of Eu^{3+} in sol-gel produced γ-Al_2O_3. Photoinduced rearrangements of nanocrystals enhanced by localization of the excitation energy can produce persistent spectral holes for Eu^{3+}. The special vibrational properties of size-restricted crystals lead to a modified density of states which is manifested in a nearly exponential temperature dependence of the transient spectral hole widths.

ACKNOWLEDGMENTS

We thank T. N. Vasilevskaya for the XRD determination of the nanoparticle size. Support by the U.S. NSF (Grants Nos. DMR-9307610 and DMR-9321052), the Russian RBRF (Grant No. 93-02-2560), and the ISF (Grant Nos. NUC000 and NUC300) is gratefully acknowledged.

[1] R. Vacher and E. Courtens, in *Phonons-89*, edited by S. Hunklinger, W. Ludwig, and G. Weiss (World Scientific, Singapore, 1990), Vol. 1, p. 635.
[2] A. Tamura and T. Ichinokava, J. Phys. C **16**, 4779 (1983).
[3] J. Dumas, J. Serughetti, J. L. Rouseet, A. Boukenter, B. Champagnon, E. Duval, and J. F. Quinson, J. Non-Cryst. Solids **121**, 128 (1990); T. Woignier, J. L. Sauvajol, J. Pelous, and R. Vacher, *ibid.* **121**, 206 (1990).
[4] R. M. Macfarlane and R. M. Shelby, J. Lumin. **36**, 179 (1987).
[5] K. W. Jang and R. S. Meltzer, Phys. Rev. B **52**, 6431 (1995).
[6] S. P. Feofilov, A. A. Kaplyanskii, and R. I. Zakharchenya, J. Lumin. **66/67**, 349 (1996).
[7] B. E. Yoldas, Am. Ceram. Soc. Bull. **54**, 286 (1975).
[8] R. I. Zakharchenya and T. N. Vasilevskaya, J. Mater. Sci. **29**, 2806 (1994).
[9] Th. Schmidt, R. M. Macfarlane, and S. Völker, Phys. Rev. B **50**, 15 707 (1994).
[10] R. M. Macfarlane and R. M. Shelby, in *Spectroscopy of Solids Containing Rare-Earth Ions*, edited by A. A. Kaplyanskii and R. M. Macfarlane (North-Holland, Amsterdam, 1987), p. 51.
[11] K. Tanaka, T. Okuno, H. Yugami, M. Ishigami, and T. Suemoto, Opt. Commun. **86**, 45 (1991).
[12] K. Koyama and T. Suemoto, J. Lumin. **66/67**, 164 (1996).
[13] W. R. Babbit, A. Lezama, and T. W. Mossberg, Phys. Rev. B **39**, 1987 (1989).
[14] D. L. Huber, J. Non-Cryst. Solids **51**, 241 (1982).
[15] A. Tamura, Phys. Rev. B **52**, 2668 (1995).
[16] F. J. Bergin, J. F. Donegan, T. J. Glynn, and G. F. Imbush, J. Lumin. **34**, 307 (1986).
[17] B. Sauter, Th. Basché, and C. Bräuchle, J. Opt. Soc. Am. B **9**, 804 (1992).
[18] W. H. Hesselink and A. Wiersma, J. Chem. Phys. **73**, 648 (1980).